Hindawi Publishing Corporation
International Journal of Photoenergy
Volume 2008, Article ID 739864, 7 pages
doi:10.1155/2008/739864

Research Article

Photoelectrochemical Characterization of Sprayed α-Fe_2O_3 Thin Films: Influence of Si Doping and SnO_2 Interfacial Layer

Yongqi Liang, Cristina S. Enache, and Roel van de Krol

Department DelftChemTech/Materials for Energy Conversion and Storage, Faculty of Applied Sciences, Delft University of Technology, P.O. Box 5045, 2600 GA Delft, The Netherlands

Correspondence should be addressed to Yongqi Liang, y.liang@tudelft.nl

Received 24 July 2007; Accepted 20 December 2007

Recommended by Russell Howe

α-Fe_2O_3 thin film photoanodes for solar water splitting were prepared by spray pyrolysis of $Fe(AcAc)_3$. The donor density in the Fe_2O_3 films could be tuned between 10^{17}–10^{20} cm^{-3} by doping with silicon. By depositing a 5 nm SnO_2 interfacial layer between the Fe_2O_3 films and the transparent conducting substrates, both the reproducibility and the photocurrent can be enhanced. The effects of Si doping and the presence of the SnO_2 interfacial layer were systematically studied. The highest photoresponse is obtained for Fe_2O_3 doped with 0.2% Si, resulting in a photocurrent of 0.37 mA/cm^2 at 1.23 V_{RHE} in a 1.0 M KOH solution under 80 mW/cm^2 AM1.5 illumination.

1. INTRODUCTION

Not long after the first report of stable photoelectrochemical O_2 evolution on single crystalline TiO_2 [1], significant research efforts were made to search for new oxide materials with smaller bandgaps to enhance visible light absorption [2]. Fe_2O_3 stands out with its nearly ideal bandgap of 2.2 eV [3] and its high-photochemical stability in aqueous solutions [4]. Though high-photoconversion efficiencies were already shown for polycrystalline Fe_2O_3 pellets [5] and single crystalline Fe_2O_3 samples [6], thin films are generally preferred in order to avoid the high resistivities encountered in, for example, single crystals, and to reduce the cost for fabrication. Very recently, an exceptionally high photocurrent of 2.7 mA/cm^2 at a bias of 1.23 V relative to the reversible hydrogen electrode (RHE) under simulated AM1.5 sunlight was reported for porous films synthesized using atmospheric pressure chemical vapor deposition (APCVD) [7]. While this breakthrough represents a major step forward, practical applications still require an additional ~4 times improvement in photocurrent. In order to achieve this, more detailed insights into the origin of the high photoresponse are required.

The key ingredients for the high performance of the APCVD films seem to be (i) Si doping, which is thought to induce a favorable morphology during film growth [8], (ii) the presence of a thin SiO_2 interfacial layer between the Fe_2O_3 and the transparent conducting substrate [7], and (iii) the addition of a cobalt catalyst [7]. The aim of the present study is to reveal the effects of Si doping and the addition of a thin interfacial layer (in this case SnO_2) between the transparent conducting substrate (TCO) and the Fe_2O_3. Toward this end, thin dense undoped and Si-doped Fe_2O_3 films are deposited onto conductive glass substrates by spray pyrolysis. Although spray pyrolysis will not generally yield the high degree of texturing that is required for optimal performance, the ease of doping and smooth film morphology greatly simplifies the photoelectrochemical characterization of the material. The photoresponse and the electrical characteristics of the deposited films are studied for various Si concentrations and the effect of a thin SnO_2 interfacial film is investigated.

2. EXPERIMENTAL

Thin films of α-Fe_2O_3 (hematite) were prepared by spray pyrolysis of a 0.04 M $Fe(AcAc)_3$ (Alfa Aesar, Karlsruhe, Germany) solution in a mixed solvent (2 : 1) of ethyl acetate and ethanol. To avoid large fluctuations of the temperature during spraying and to give the solvent enough

time to evaporate, the spray pyrolysis was carried out using 15 seconds on cycle, 45 seconds off cycle. Compressed air was used as the carrier gas.

Silicon doping was achieved by addition of different amounts of TEOS (99.9%, Alfa Aesar, Karlsruhe, Germany) to the precursor solution. All the Si concentrations mentioned hereafter refer to the atomic Si : Fe ratio in the spray solution, though the Si concentration that actually ends up in the deposited Fe_2O_3 films may be somewhat different. The SnO_2 interfacial layer was deposited by spray pyrolysis of a 0.1 M $SnCl_4$ (99%, Acros organics, NJ, USA) solution in ethyl acetate (99.5%, J. T. Baker, Deventer, Holland).

FTO glass (SnO_2:F, TEC-15, Libbey-Owens-Ford, Hartford, IN, USA, 2.5-mm thick) was used as a transparent conducting substrate for photoelectrochemical experiments. Fused silica (ESCO, S1-UV grade, thickness of 1 mm) was used as a substrate for the film thickness determination by UV-vis absorption measurements. All the substrates were cleaned by ultrasonic rinsing in pure ethanol, and subsequently dried under N_2 flow. During deposition, the substrate was heated using a temperature-controlled hotplate.

Structural characterization of the films was carried out using a Bruker D8 Advance X-ray diffractometer in the grazing incidence mode. A Renishaw 1000 spectrometer was used for microscopic Raman analysis.

To determine the film thickness, UV-vis absorption spectra of the SnO_2 and Fe_2O_3 films on fused silica were measured with a Lambda 900 UV-vis spectrophotometer (Perkin Elmer). For the Fe_2O_3 films, the thickness was further verified by inspection of the cross-section of the films using a JSM-6500F field emission scanning electron microscope (SEM).

A home-made three-electrode electrochemical cell, fitted with a fused silica window, was used for photoelectrochemical characterization. An aqueous solution of 1.0 M KOH (pH 14) was used as the electrolyte. The potential of the Fe_2O_3 working electrode (area: 0.283 cm^2) was controlled by a potentiostat (EG&G PAR 283), which was combined with a frequency response analyzer (Solartron 1255, Schlumberger, Hampshire, England) for impedance analysis. An Ag/AgCl electrode (REF321, Radiometer Analytical, Villeurbanne, France) was used as a reference and a coiled Pt wire was adopted as the counter electrode. All the potentials mentioned in this article are referred to Ag/AgCl (0.208 V versus NHE at 25°C), unless stated otherwise.

For spectral response measurements, light from a 200 W tungsten halogen lamp was coupled into a grating monochromator (Acton SpectraPro 150i) via a 50-mm diameter fused silica lens. Between the monochromator and the sample, an electronic shutter (Uniblitz LS6) was placed, and high-pass colored glass filters (Schott, 2×3 mm) were used to remove second-order diffracted light. The intensity of the monochromatic light was measured with a calibrated photodiode (Ophir, Jerusalem, Israel, PD300-UV). For white-light measurements, a solar simulator (EPS 1200S, KH Steuernagel Lichttechnik GmbH, Mörfelden-Walldorf, Germany) was used to provide simulated AM1.5 sunlight. The light from the solar simulator was directed to the sample by mirror (UV-enhanced aluminum, Melles Griot, Cambridge, England) placed under a 45° angle. This resulted in an illumination intensity of 80 mW/cm^2 (i.e., 80% of AM1.5 light) at the position of the sample, as measured with a calibrated Si photodiode. An AM1.5 standard spectrum reported by NREL [9] was used for integrating the monochromatic photocurrent and comparing it to the white light response.

3. RESULTS AND DISCUSSION

Figure 1(a) shows X-ray diffraction results for the 0.1% Si-doped Fe_2O_3 films. At 350°C, the peak intensity distribution corresponds to that of regular polycrystalline hematite. As the temperature is increased, the intensity of the (110) diffraction peak becomes stronger, while the (104) diffraction becomes less pronounced. For the samples without Si dopant, the same trend is observed. Hence, (110) is preferred growth direction for sprayed Fe_2O_3 films at deposition temperatures of 400°C and higher.

The preferred (110) orientation implies that the c-axes of the crystal domains in the Fe_2O_3 film are parallel to the substrate surface. Since electron transport along the c-axis is known to be about four orders of magnitude slower than in the other directions [10, 11], the (110) orientation observed here is much more favorable for electron transport than the (001) oriented hematite films deposited with, for example, ion-beam assisted CVD [12]. Moreover, the conductivity along the c-axis has been suggested to be p-type in character [13, 14]. This implies that a (110) preferred orientation would also be favorable for photoanodes made of vertically aligned hematite nanowires, where efficient hole transport in the direction parallel to the substrate is desired.

In addition to the hematite peaks, two other phases seem to be present in minor amounts as indicated by small peaks at 29.8° and 32.1°. The small peak at 29.8°, which is attributed to the presence of Fe_3O_4 [15], appears only in the samples deposited at low temperatures (≤450°C). The origin of the peak at 32.1° is not yet clear and can not be attributed to any of the known iron oxides. The closest candidate would be β-Fe_2O_3 with a peak at 32.9°, but this seems to be too far from the observed peak position. Moreover, β-Fe_2O_3 has been reported to disappear after annealing at high temperatures (550°C) [16], whereas Figure 1(a) shows the peak at 32.9° to actually increase with temperature.

Figure 1(b) shows the Raman spectra of Fe_2O_3 doped with 0.2% Si. Compared to the α-Fe_2O_3 peaks, the intensity of the Fe_3O_4 peak at 656 cm^{-1} [17] decreases with increasing deposition temperature. This is consistent with the XRD results in Figure 1(a), and supports our conclusion that Fe_3O_4 is only formed at temperatures ≤450°C under the currently used conditions for spray pyrolysis.

As can be observed in Figures 1(c) and 1(d), spray pyrolysis of the $Fe(AcAc)_3$ solution yields compact films of uniform thickness. A thickness of 200 nm was reached after 40 spray cycles (each cycle consists of 15 seconds spray on +45 seconds spray off), resulting in an average deposition rate of 20 nm/min for spraying at 450°C. No significant differences

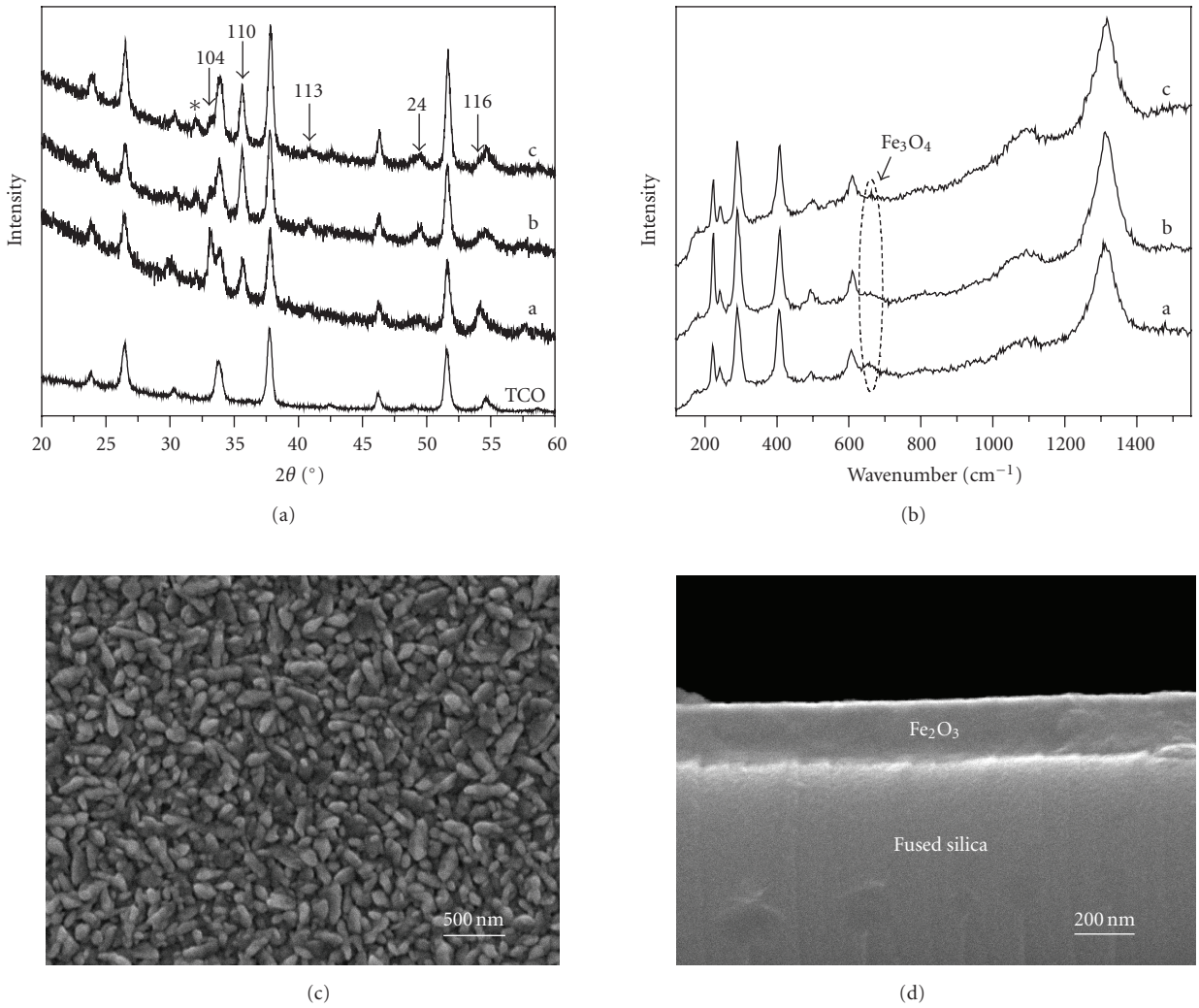

FIGURE 1: (a) XRD of Fe_2O_3 films doped with 0.1% Si deposited at (a) 350°C, (b) 400°C, (c) 450°C. The diffraction pattern of the TCO substrate fired at 400°C in the air is also shown for comparison. Undefined peaks are marked with *. (b) Raman spectra of Fe_2O_3 samples doped with 0.2% Si deposited at (a) 350°C, (b) 450°C, (c) 500°C. (c) SEM micrographs showing the typical morphology of the Fe_2O_3 films on TCO. (d) Cross-section of a 200 nm Fe_2O_3 film on a fused silica substrate.

in film morphology are observed between undoped and Si-doped films.

Figure 2(a) shows the measured photocurrent versus potential curves for Fe_2O_3 films doped with 0.2% Si. Comparison between curves a and b shows a significant improvement of the photocurrent response, when a 5 nm SnO_2 interfacial layer is present between the TCO substrate and the Fe_2O_3 film. This improvement is especially pronounced at lower potentials. Specifically, at a potential of 0.23 V versus Ag/AgCl, which corresponds to a reversible hydrogen potential of 1.23 V_{RHE}, the photocurrent increases from 0.04 mA/cm^2 to 0.33 mA/cm^2. In fact, Figure 2(a) shows that the interfacial layer shifts the photocurrent onset potential by ~0.2 V in the cathodic direction. Another effect of the interfacial layer is a significant improvement of the reproducibility of the photoresponse, especially for undoped samples. Without the interfacial layer, photocurrent variations of up to a factor of five or more are observed between samples made under the same conditions. With the interfacial layer, these variations are within a factor of 2.

For the Si-doped samples, front-side (electrolyte-side) illumination (curve a in Figure 2(a)) always gives a higher photocurrent than back-side (substrate-side) illumination (curve a' in Figure 2(a)). This shows that the rate-limiting step in the Si-doped samples is hole transport. In contrast, electron transport is found to be rate limiting in undoped Fe_2O_3 samples. The introduction of the SnO_2 interfacial layer does not change the ratio between the front-side photocurrent and the back-side photocurrent (curves b and b'). Since front-side illumination shows higher photocurrents, all the data discussed from this point forward are measured using front-side illumination.

The thickness of the SnO_2 films was determined by UV-vis absorption measurements, corrected for reflection, assuming an absorption coefficient of 1.3×10^5 cm^{-1} at 300 nm [18]. For these measurements, the SnO_2 films were

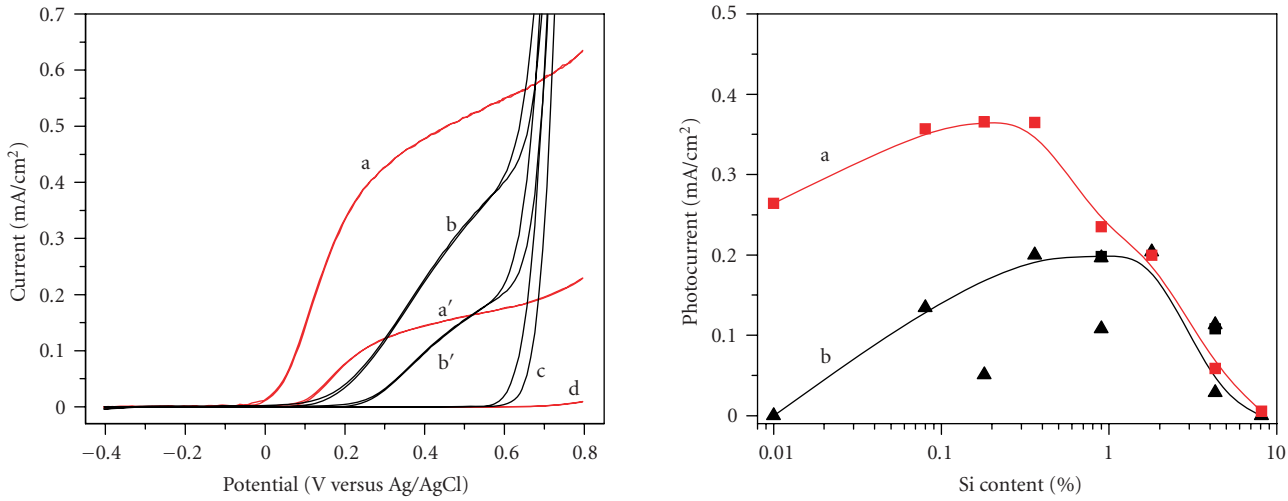

Figure 2: (a) Current-potential measurements under simulated 80 mW/cm^2 AM1.5 sunlight for Fe_2O_3 doped with 0.2% Si with (a: front-side illumination; a': back-side illumination; d: dark) and without (b: front-side illumination; b': back-side illumination; c: dark) 5 nm SnO_2 interfacial layer. The scan rate is 20 mV/s. (b) Dependence of the photocurrent (front-side illumination) at 0.23 V versus Ag/AgCl on the Si dopant concentration; a: with SnO_2 interfacial layer; b: without SnO_2 interfacial layer.

deposited on fused silica substrates, and the growth rate was assumed to be similar to that on the TCO substrates. Because of the small thickness (~5 nm) and the large bandgap (>3.6 eV) of SnO_2, it can be safely assumed that the contribution of the interfacial layer to the photocurrent is negligible. Furthermore, X-ray diffraction revealed that the SnO_2 interfacial layer does not affect the preferred orientation of the Fe_2O_3 films.

Figure 2(b) shows the photocurrent at 0.23 V versus Ag/AgCl for Fe_2O_3 films with various amounts of Si doping. For the films without SnO_2 interfacial layer, the optimum Si concentration is ~1%, whereas an optimum concentration range between 0.2 and –0.4% is found for films with an interfacial SnO_2 layer. It should be noted that these concentrations are much lower than in previously reported studies on Si-doped Fe_2O_3 [19, 20], where a significant fraction of Si content was presumably present as a second phase. As can be seen in Figure 2(b), the presence of an SnO_2 interfacial layer is especially beneficial at low-Si concentrations.

Previous reports have shown that unintentional incorporation of donor-type species may also be responsible for improved photoefficiencies. Examples of impurities that are sometimes difficult to avoid are Si [8, 19], carbon in the case of organic Fe-precursors such as $Fe(AcAc)_3$, and chlorine when $FeCl_3$ or $FeCl_2$ are used as precursors [7]. The electrical conductivity can also be affected by the presence of other iron oxide phases, such as FeO, Fe_3O_4, or Fe_2O_3, which may be formed depending on the deposition conditions and the presence of trace impurities [2, 16, 17].

To rule out that the beneficial effect of the SnO_2 layer is caused by the diffusion of Sn into the Fe_2O_3 film (i.e., unintentional doping), a Mott-Schottky analysis was carried out. Figure 3(a) shows a Mott-Schottky plot of an undoped Fe_2O_3 film recorded in the dark. The presence of a 5 nm SnO_2 interfacial layer has no significant effect on the curve, which already indicates that no significant Sn diffusion into the Fe_2O_3 layer occurs. According to the depletion layer model, the capacitance of the semiconductor space charge layer C_{sc} changes with the applied potential V_A according to the Mott-Schottky equation,

$$\frac{1}{C_{sc}^2} = \frac{2}{e\varepsilon_r\varepsilon_0 N_d A^2}\left(V_A - V_{fb} - \frac{kT}{e}\right), \quad (1)$$

where ε_r is the semiconductor dielectric constant, A is the surface area of the electrode, N_d is the donor density, and V_{fb} is the flatband potential. At potentials positive of −0.6 V, the Fe_2O_3 is fully depleted and the slope of the curve reflects the donor density in the conducting FTO substrate. From the intercept of the dashed lines in Figure 3(a) and the dielectric constant of 80 for Fe_2O_3 [22], the film thickness is calculated according to $C = \varepsilon_0\varepsilon_r A/d$, yielding a thickness value of 135 nm. The discrepancy between the calculated value and the value determined from the SEM cross-section (200 nm, Figure 1(d)) is presumably caused by the surface roughness and/or the frequency dispersion in the Mott-Schottky plots, which will be discussed in more detail below. A donor density of 1.2×10^{17} cm^{-3} in the Fe_2O_3 is calculated from the slope of the Mott-Schottky plot between −0.8 V and −0.6 V. This value is quite small for a semiconducting metal oxide indicating that (i) the sprayed Fe_2O_3 films are of high quality with relatively few electronic defects and (ii) little, if any, Sn diffuses from either the interfacial layer or the F:SnO_2 conducting substrate into the Fe_2O_3 film. The beneficial effect of the SnO_2 interfacial layer is tentatively attributed either to the passivation of surface states or to an improvement of the band alignment between the Fe_2O_3 and the underlying TCO.

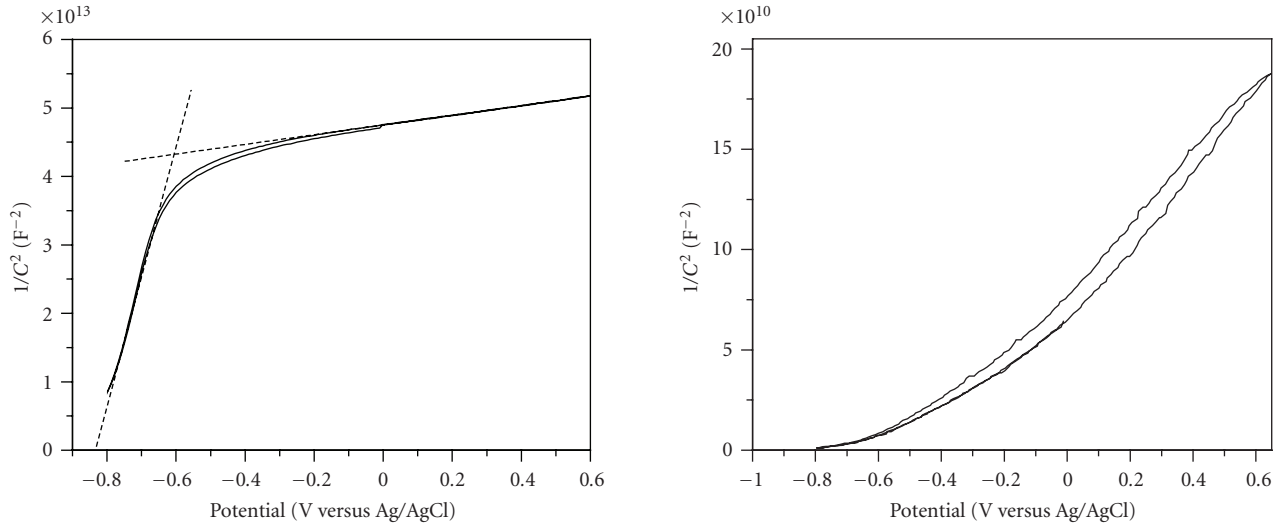

Figure 3: Mott-Schottky measurement of Fe_2O_3 films (a) undoped, measured at 30 kHz and (b) doped with 0.9% Si, measured at 1 kHz. The frequency was selected based on the impedance spectra (not shown), in the range where the slope of $\log|-Z''|$ versus $\log(\omega)$ is close to -1, and the real part of impedance is more or less constant [21].

After introducing 0.9% Si dopant in the precursor solution, dramatic changes in the Mott-Schottky plot are observed (Figure 3(b)). From these data, a donor density of $1 \times 10^{20}\,\text{cm}^{-3}$ is calculated. However, considering the roughness of the surface on a microscopic scale and the fact that the depletion layer extends only a few nanometers into the Fe_2O_3 film, the effective surface area will be larger than the geometrical area. As a result, the true donor density will be somewhat smaller than the calculated value. The fact that the curve concaves upwards in Figure 3(b) supports the interpretation in terms of surface roughness effects [23]. If all Si atoms present in the precursor solution are incorporated into the film and act as ionized donors, a maximum donor density of $4 \times 10^{20}\,\text{cm}^{-3}$ is expected. This is within the same order of magnitude as the measured donor density, indicating that a significant fraction of the Si atoms, is incorporated into the film where they indeed act as ionized donors. This is a somewhat unexpected result, since the pyrolysis of TEOS usually requires temperatures much higher than 450°C [7].

Another important parameter of the semiconductor that can be derived from Mott-Schottky measurements is the flat band potential. Although the flat band potential depends on the exposed crystal plane and on the donor density inside the Fe_2O_3, most reports agree that the flat band potential of Fe_2O_3 with a donor density of $\sim 10^{17}\,\text{cm}^{-3}$ is -0.7 V in a 1.0 M KOH solution [6, 24]. A somewhat more negative potential of -0.84 V versus Ag/AgCl is found for our spray-deposited undoped Fe_2O_3 films (Figure 3(a)). However, it should be mentioned that an accurate determination of the flat band potential is complicated by some degree of frequency dispersion observed in the Mott-Schottky plots [25, 26]. Specifically, in the frequency range between 1 kHz and 30 kHz, the flat band potential varies between -0.67 V and -0.96 V. The donor density shows much less variation; values between $1.3 \times 10^{17}\,\text{cm}^{-3}$ and $0.8 \times 10^{17}\,\text{cm}^{-3}$ are observed between 1 and 30 kHz. A more detailed analysis of the impedance spectra to elucidate the origin of the frequency dispersion is still ongoing, but is complicated by the fact that the equivalent circuits that are normally used to model semiconducting photoanodes are not able to describe the measured data in a satisfactory manner.

To objectively compare the photoelectrochemical performance of our films with the literature, the incidented photon-to-current conversion efficiency (IPCE) has been measured as a function of wavelength. The IPCE of the Fe_2O_3 films doped with 0.1% Si and deposited on top of a 5 nm SnO_2 interfacial layer is shown in Figure 4(a). A bias of 0.4 V versus Ag/AgCl was used, since no accurate steady-state photocurrent values could be obtained at more negative potentials due to a transient response when the light is switched on and off. A maximum IPCE of 20% is found at 370 nm, which is comparable to the best spray-deposited Fe_2O_3 samples reported so far [16], though still a factor of about 2.5 below the samples made by APCVD [7]. At wavelengths shorter than 370 nm, however, the IPCE shows a steeper decrease than that reported in the literature for Fe_2O_3 [7, 16]. While the origin of this difference is not clear, it does explain the relatively modest response of our samples to white-light illumination.

To compare the IPCE spectra with the photoresponse under simulated AM1.5 sunlight, the IPCE data are integrated over the standard AM1.5 solar spectrum and corrected for an actual intensity of $80\,\text{mW/cm}^2$ (Figure 4(b)). The photocurrent is assumed to depend linearly on the light intensity, which is reasonable for the low-light intensities used in this study (10–20 $\mu\text{W/cm}^2$). The integrated photocurrent of $0.53\,\text{mA/cm}^2$ is higher

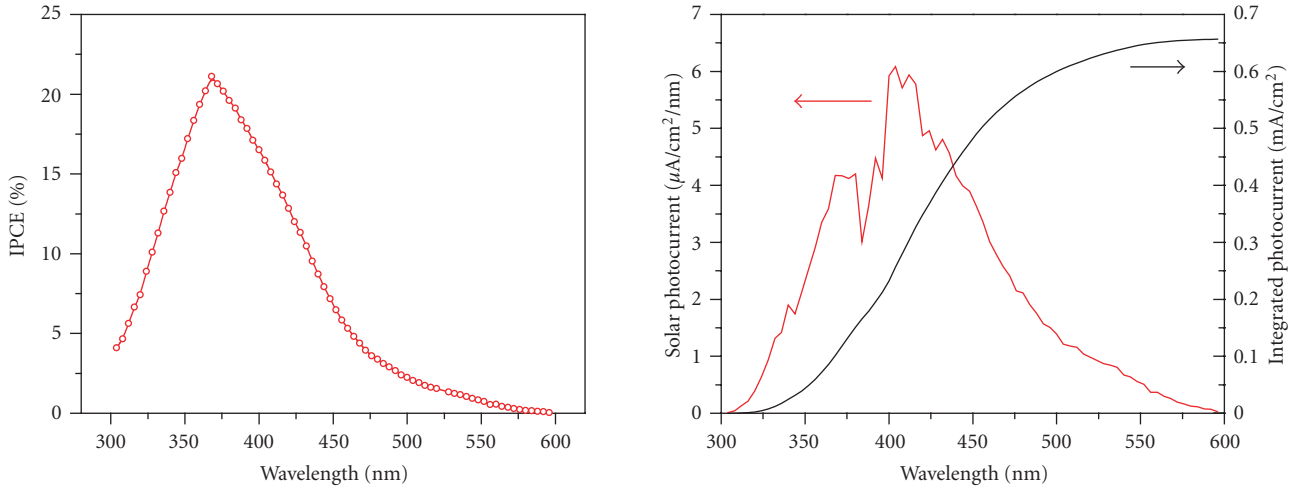

FIGURE 4: (a) IPCE curve for 0.1% Si-doped Fe_2O_3 measured at 0.4 V versus Ag/AgCl. (b) Momentary and integrated solar photocurrent of the sample obtained by multiplying IPCE with the photon flux spectrum of AM1.5 sunlight. When correcting for the actual experimental intensity of 80 mW/cm^2, an integrated photocurrent of $0.8 \times 0.66 = 0.53$ mA/cm^2 is obtained.

than the measured AM1.5 photocurrent of 0.44 mA/cm^2 (Figure 2(a)). Although the reason for this discrepancy is not yet clear, this perhaps rather conservative value for the photoresponse under simulated AM1.5 light is much better suited for comparison with results from other labs than the often reported photocurrents measured with xenon light sources. As pointed out recently by Murphy et al., the high-UV content of xenon lamps often leads to severe overestimation of the photoconversion efficiencies [3].

4. CONCLUSIONS

Thin-film hematite Fe_2O_3 photoanodes were deposited on transparent conducting glass substrates by spray pyrolysis. A thin, 5 nm SnO_2 interfacial layer between the Fe_2O_3 and TCO glass was found to be beneficial for both the reproducibility and the photocurrent efficiency of the Fe_2O_3 films. While the beneficial effect of an interfacial layer on the photoresponse of Fe_2O_3 has been previously reported for ultrathin (~1 nm) SiO_2 films, in this study we show that the beneficial effect of such an interfacial layer is not limited to the material SiO_2, and that electrons do not need to be able to tunnel through the interfacial layer. Silicon concentrations between 0.2 and 0.4% are found to give the highest photocurrents for spray-deposited Fe_2O_3 films. The highest photoresponse measured during this study was 0.37 mA/cm^2 at 0.23 V versus Ag/AgCl (1.23 V versus RHE) under 80 mW/cm^2 AM1.5 illumination for films doped with 0.2% Si and deposited on a 5 nm SnO_2 interfacial layer. Since hole transport is the rate limiting factor for these films, further improvements of the efficiency requires nanostructured electrodes with high aspect ratios in order to minimize the distance that the photogenerated holes have to travel before reaching the semiconductor/electrolyte interface. Development of suitable low-cost deposition techniques for such electrodes, that can be readily scaled-up and that allow accurate control over dopant concentrations, is one of the major challenges in the field of photocatalysis and solar water splitting.

ACKNOWLEDGMENTS

This work is financially supported under the sustainable hydrogen program (Project no. 053.61.009) by NWO-ACTS. The authors also want to express their thanks to Ilkay Cesar from EPFL for stimulating discussions on Fe_2O_3. Roel van de Krol gratefully acknowledges support from the Netherlands Organization for Scientific Research (NWO) in the form of a VENI Grant.

REFERENCES

[1] A. Fujishima and K. Honda, "Electrochemical photolysis of water at a semiconductor electrode," *Nature*, vol. 238, pp. 37–38, 1972.

[2] K. L. Hardee and A. J. Bard, "Semiconductor electrodes. X. Photoelectrochemical behavior of several polycrystalline metal oxide electrodes in aqueous solutions," *Journal of the Electrochemical Society*, vol. 124, no. 2, pp. 215–224, 1977.

[3] A. B. Murphy, P. R. F. Barnes, L. K. Randeniya, et al., "Efficiency of solar water splitting using semiconductor electrodes," *International Journal of Hydrogen Energy*, vol. 31, no. 4, pp. 1999–2017, 2006.

[4] J. H. Kennedy and M. Anderman, "Photoelectrolysis of water at α-Fe_2O_3 electrodes in acidic solution," *Journal of the Electrochemical Society*, vol. 130, no. 4, pp. 848–852, 1983.

[5] R. Shinar and J. H. Kennedy, "Photoactivity of doped α-Fe_2O_3 electrodes," *Solar Energy Materials*, vol. 6, no. 3, pp. 323–335, 1982.

[6] C. Sanchez, K. D. Sieber, and G. A. Somorjai, "The photoelectrochemistry of niobium doped α-Fe_2O_3," *Journal of Electroanalytical Chemistry*, vol. 252, no. 2, pp. 269–290, 1988.

[7] A. Kay, I. Cesar, and M. Grätzel, "New benchmark for water photooxidation by nanostructured α-Fe_2O_3 films," *Journal of*

the American Chemical Society, vol. 128, no. 49, pp. 15714–15721, 2006.

[8] I. Cesar, A. Kay, J. A. Gonzalez Martinez, and M. Grätzel, "Translucent thin film Fe_2O_3 photoanodes for efficient water splitting by sunlight: nanostructure-directing effect of Si-doping," *Journal of the American Chemical Society*, vol. 128, no. 14, pp. 4582–4583, 2006.

[9] http://rredc.nrel.gov/solar/spectra/am1.5/.

[10] T. Nakau, "Electrical conductivity of α-Fe_2O_3," *Journal of the Physical Society of Japan*, vol. 15, no. 4, p. 727, 1960.

[11] K. M. Rosso, D. M. A. Smith, and M. Dupuis, "An *ab initio* model of electron transport in hematite (α-Fe_2O_3) basal planes," *Journal of Chemical Physics*, vol. 118, no. 14, pp. 6455–6466, 2003.

[12] F. Yubero, M. Ocaña, A. Justo, L. Contreras, and A. R. González-Elipe, "Iron oxide thin films prepared by ion beam induced chemical vapor deposition: structural characterization by infrared spectroscopy," *Journal of Vacuum Science and Technology A*, vol. 18, no. 5, pp. 2244–2248, 2000.

[13] J. B. Goodenough, "Metallic oxides," *Progress in Solid State Chemistry*, vol. 5, pp. 145–398, 1971.

[14] N. Iordanova, M. Dupuis, and K. M. Rosso, "Charge transport in metal oxides: a theoretical study of hematite α-Fe_2O_3," *Journal of Chemical Physics*, vol. 122, no. 14, pp. 144305–144310, 2005.

[15] JCPDS reference card #19-0629, International Center for Diffraction Data, New York, NY, USA.

[16] C. J. Sartoretti, B. D. Alexander, R. Solarska, I. A. Rutkowska, and J. Augustynski, "Photoelectrochemical oxidation of water at transparent ferric oxide film electrodes," *Journal of Physical Chemistry B*, vol. 109, no. 28, pp. 13685–13692, 2005.

[17] A. Duret and M. Grätzel, "Visible light-induced water oxidation on mesoscopic α-Fe_2O_3 films made by ultrasonic spray pyrolysis," *Journal of Physical Chemistry B*, vol. 109, no. 36, pp. 17184–17191, 2005.

[18] K. B. Sundaram and G. K. Bhagavat, "Optical absorption studies on tin oxide films," *Journal of Physics D*, vol. 14, pp. 921–925, 1981.

[19] J. H. Kennedy, R. Shinar, and J. P. Ziegler, "α-Fe_2O_3 photoanodes doped with silicon," *Journal of the Electrochemical Society*, vol. 127, no. 10, pp. 2307–2309, 1980.

[20] C. Leygraf, M. Hendewerk, and G. A. Somorjai, "Mg- and Si-doped iron oxides for the photocatalyzed production of hydrogen from water by visible light ($2.2\,\text{eV} \leq h\nu \leq 2.7\,\text{eV}$)," *Journal of Catalysis*, vol. 78, no. 2, pp. 341–351, 1982.

[21] R. van de Krol, A. Goossens, and J. Schoonman, "Mott-Schottky analysis of nanometer-scale thin-film anatase TiO_2," *Journal of the Electrochemical Society*, vol. 144, no. 5, pp. 1723–1727, 1997.

[22] S. M. Wilhelm, K. S. Yun, L. W. Ballenger, and N. Hackerman, "Semiconductor properties of iron oxide electrodes," *Journal of the Electrochemical Society*, vol. 126, no. 3, pp. 419–424, 1979.

[23] J. Schoonman, K. Vos, and G. Blasse, "Donor densites in TiO_2 photoelectrodes," *Journal of the Electrochemical Society*, vol. 128, no. 5, pp. 1154–1157, 1981.

[24] J. H. Kennedy and K. W. Frese Jr., "Flatband potentials and donor densities of polycrystalline α-Fe_2O_3 determined from Mott-Schottky plots," *Journal of the Electrochemical Society*, vol. 125, no. 5, pp. 723–726, 1978.

[25] H. O. Finklea, "The preparation of TiO_2 electrodes with minimum Mott-Schottky frequency dispersion," *Journal of the Electrochemical Society*, vol. 129, no. 9, pp. 2003–2008, 1982.

[26] G. Oskam, D. Vanmaekelbergh, and J. J. Kelly, "A reappraisal of the frequency dependence of the impedance of semiconductor electrodes," *Journal of Electroanalytical Chemistry*, vol. 315, no. 1-2, pp. 65–85, 1991.